Guillermo Marin

Data Analytics and Visualization Group

Barcelona Supercomputing Center

Centro Nacional de Supercomputación

VIRTUAL HUMANS

Hyper-realistic visualisations of computer simulations

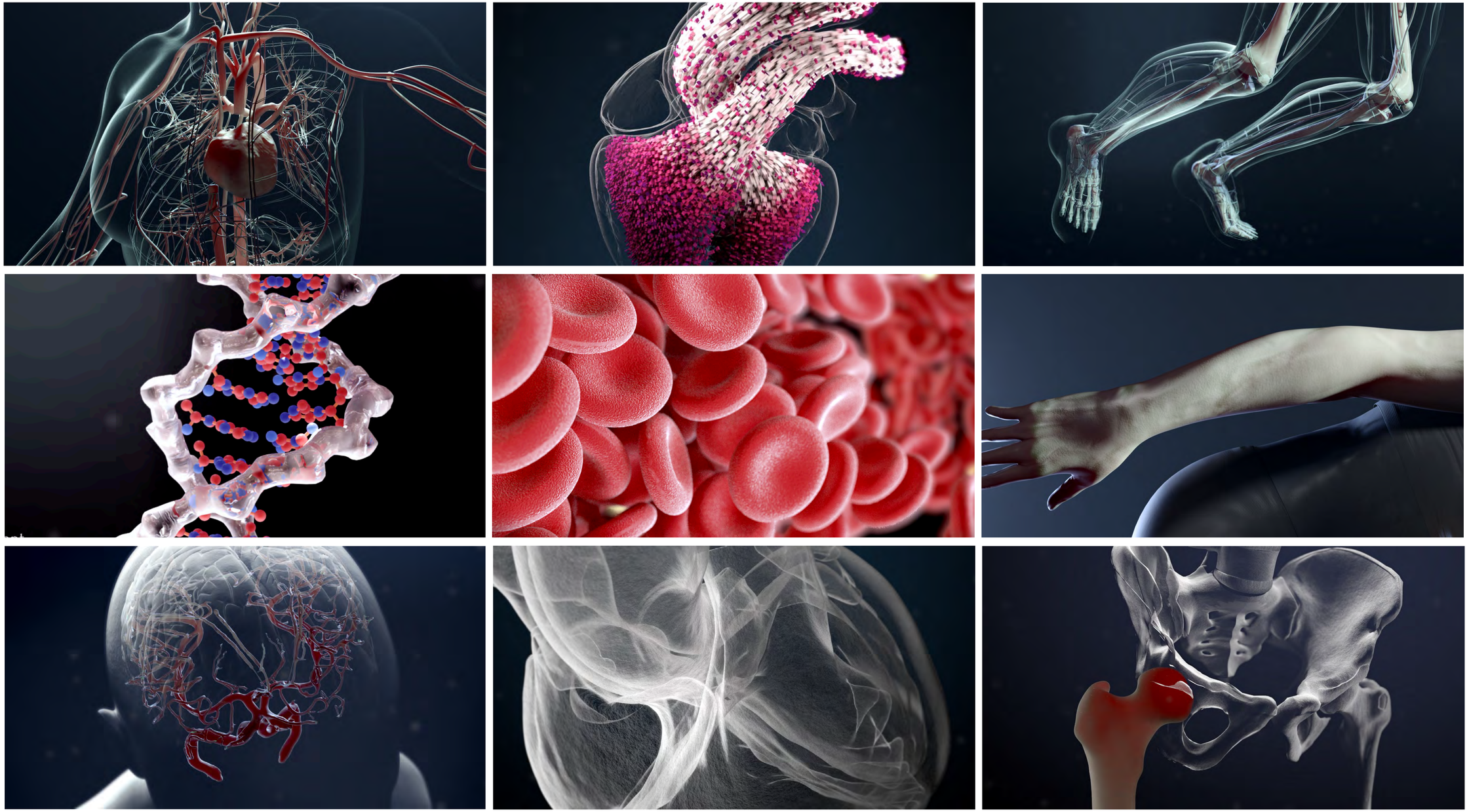

BSC-SurfSara-LRZ

~~Hyper~~-realistic visualisations of computer simulations

Photo

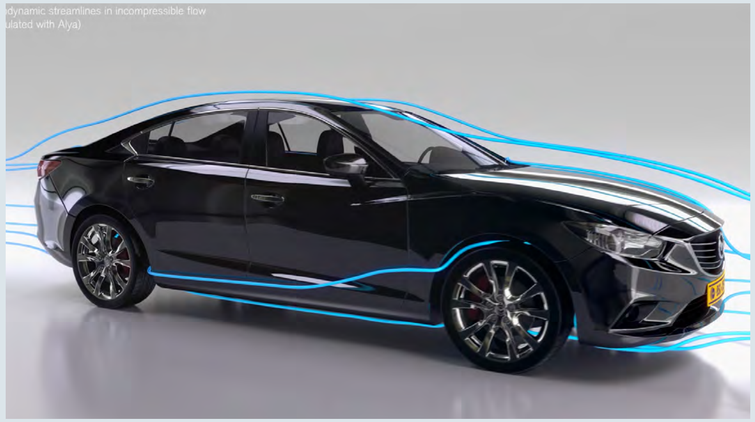

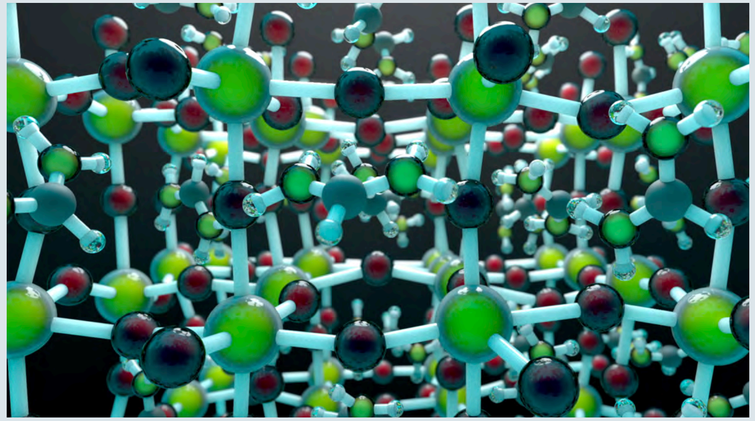

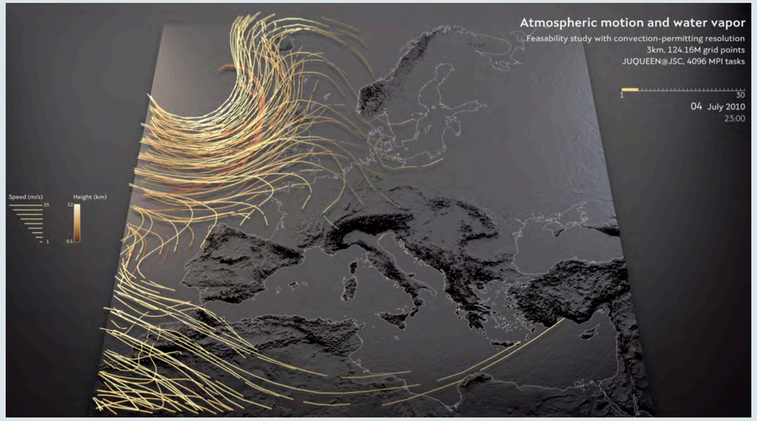

High-end visualisations of computer simulations

ALYA RED

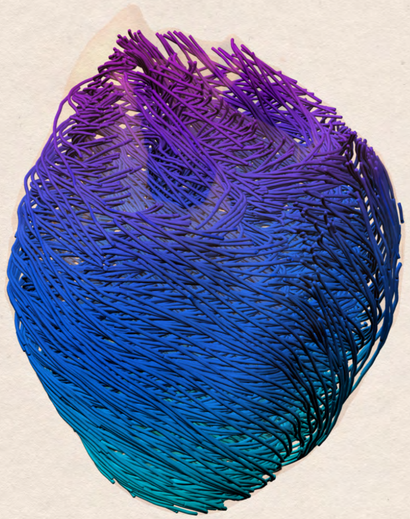

NSF

Science AAAS

ALYA RED

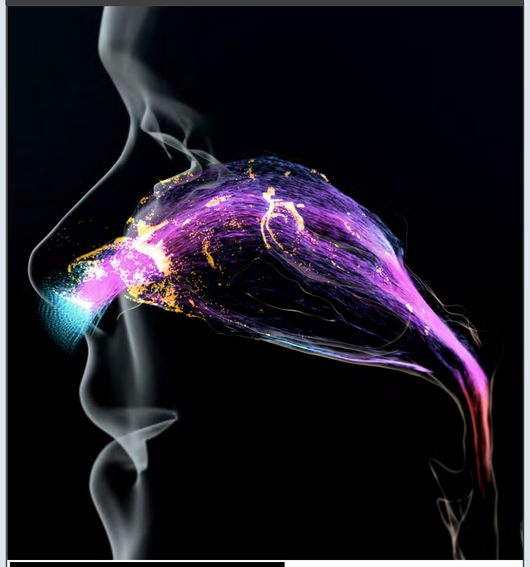

OFFICIAL SELECTION 8th ANNUAL imagine SCIENCE Film Festival

SC15 Austin, TX | hpc transforms.

CAMPANIAN IGNIMBRITE

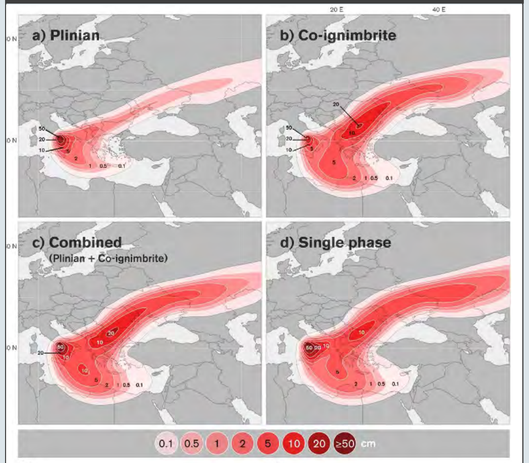

Scientific Reports **6**, Article number: 21220 (2016)

Super nice visualisations of computer simulations

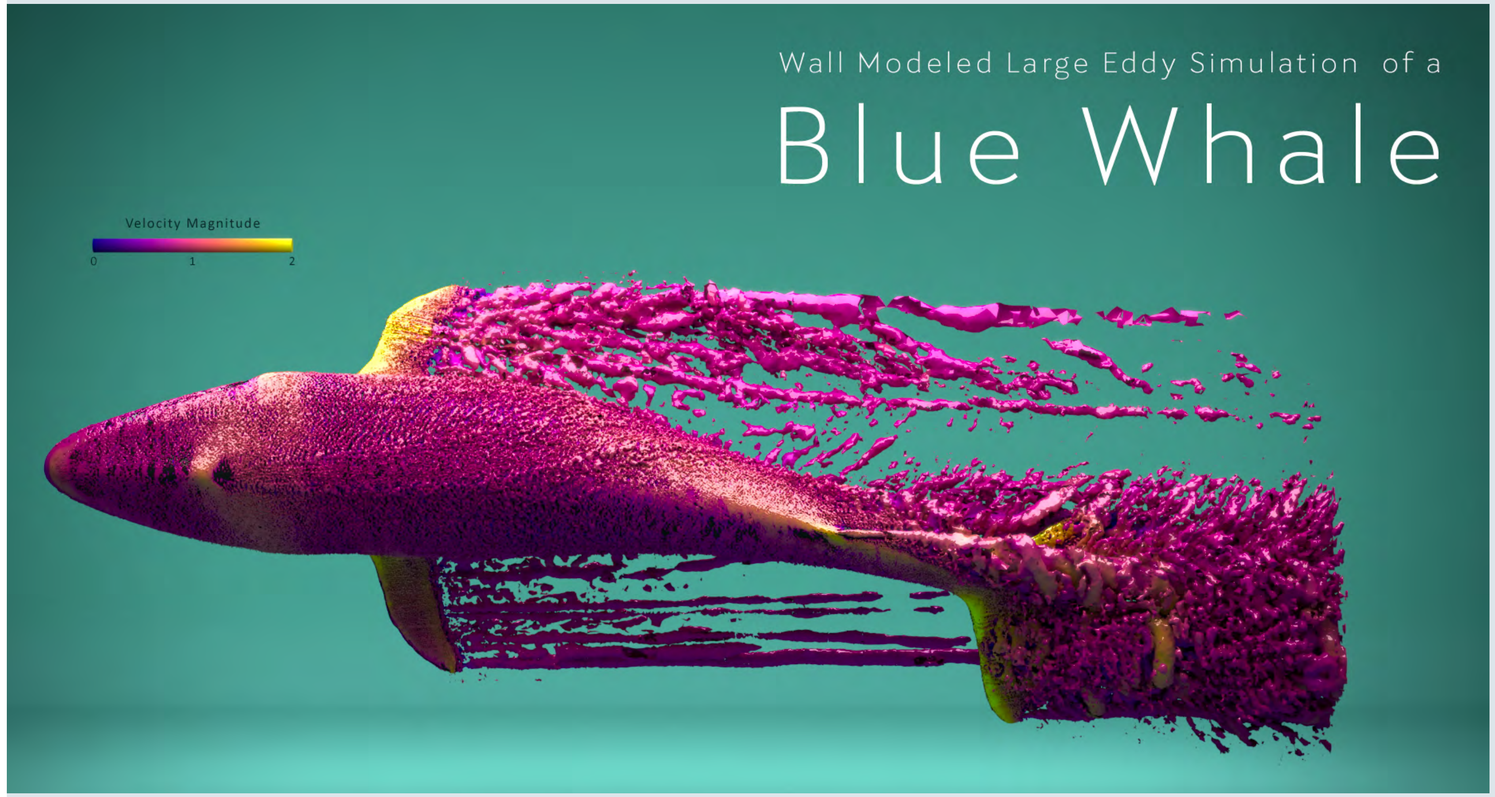

BSC Viz Team

What we do

Photo-real renders of **DATA**

Used in short movies and still images

For general public and/or peers

&

Why we do it

Maximise impact

Increase memorability

Bateman, Useful junk?, 2573-2582

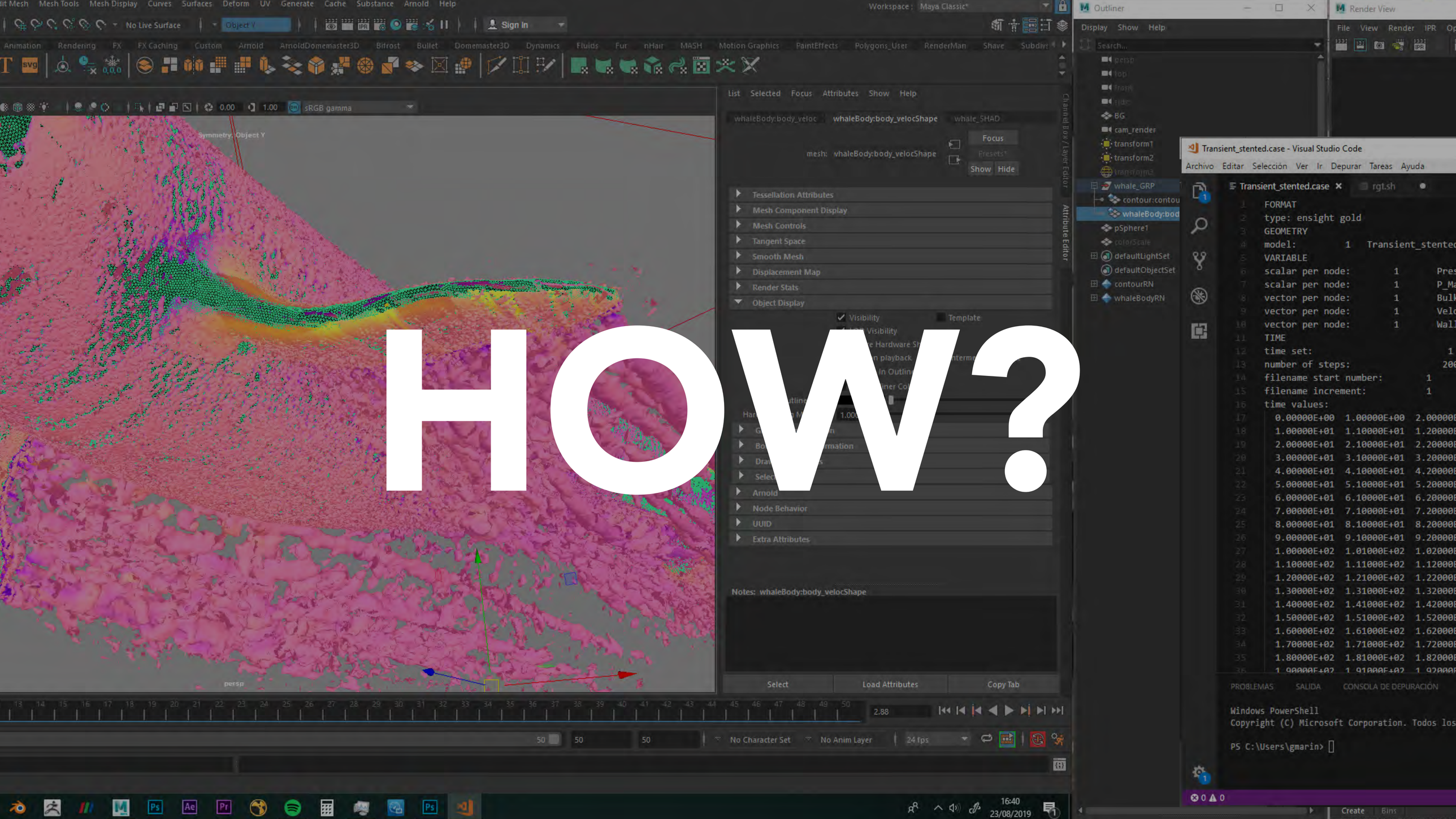
HOW?

Film industry **tools** are amazing

Film industry **people** too

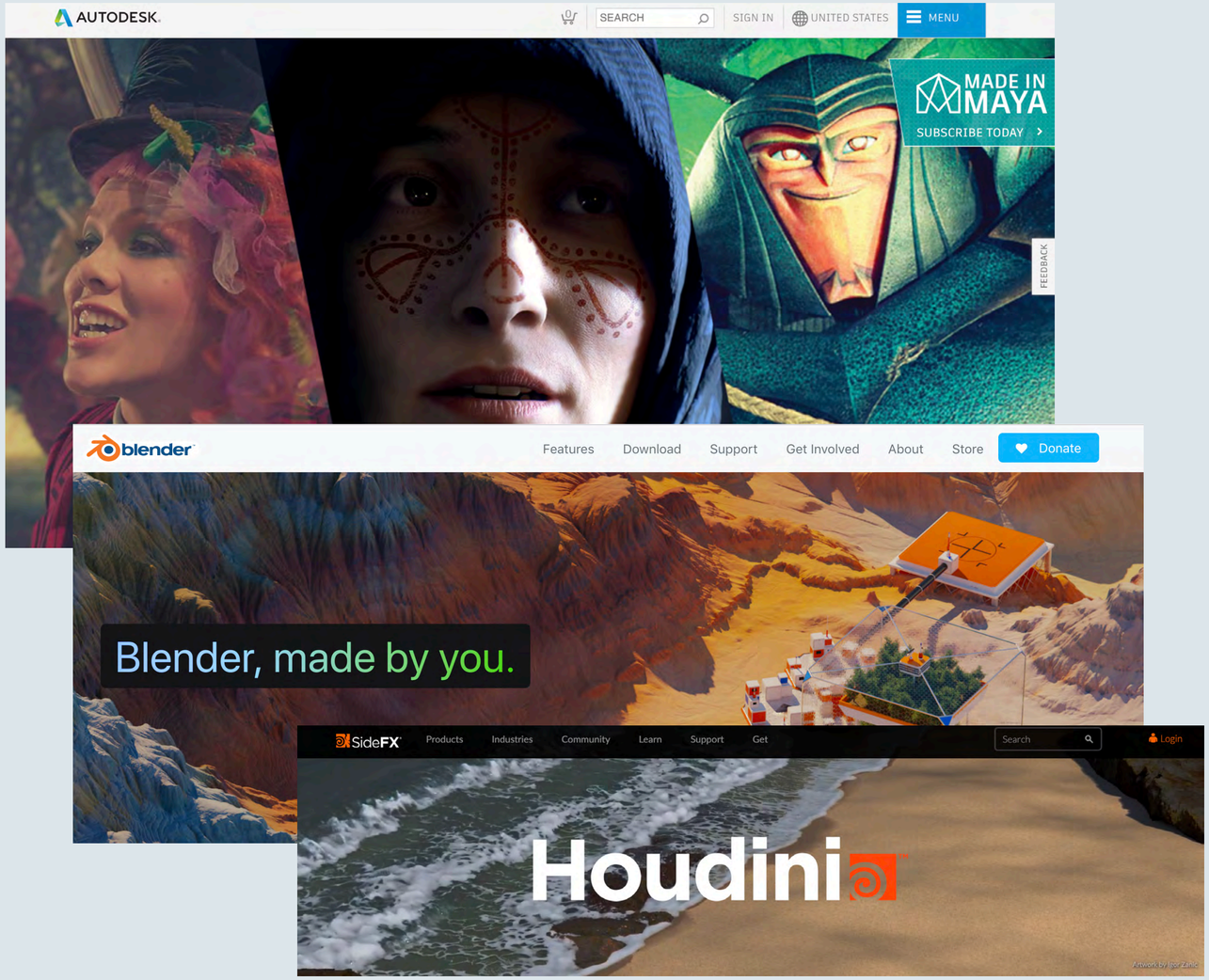

To achieve it, we need artist level of control over camera, light, textures, animation, and render quality

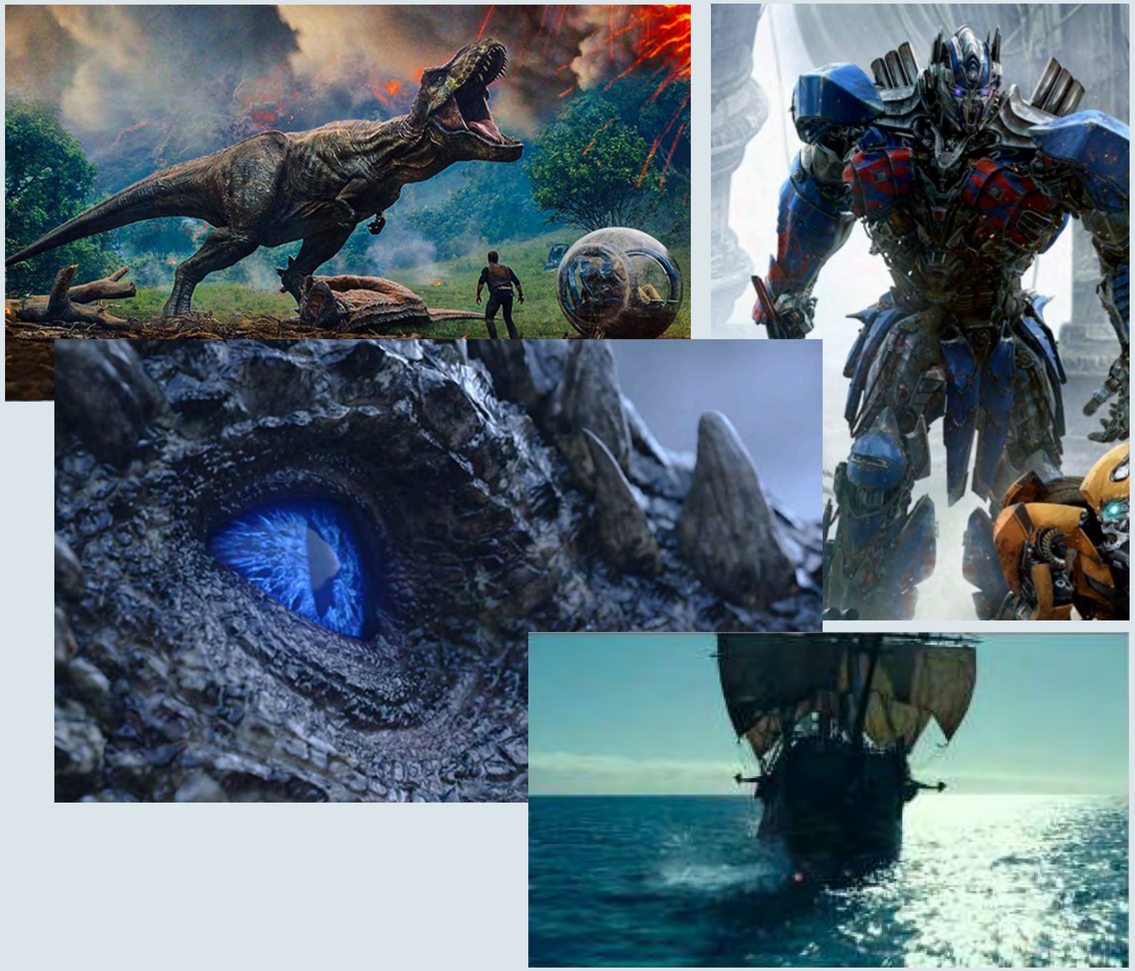

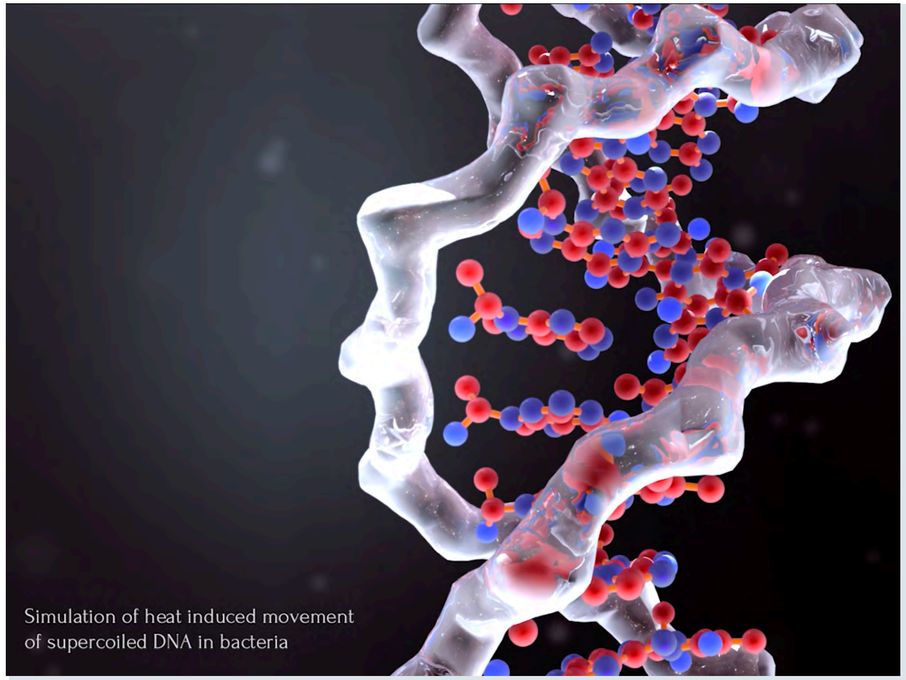

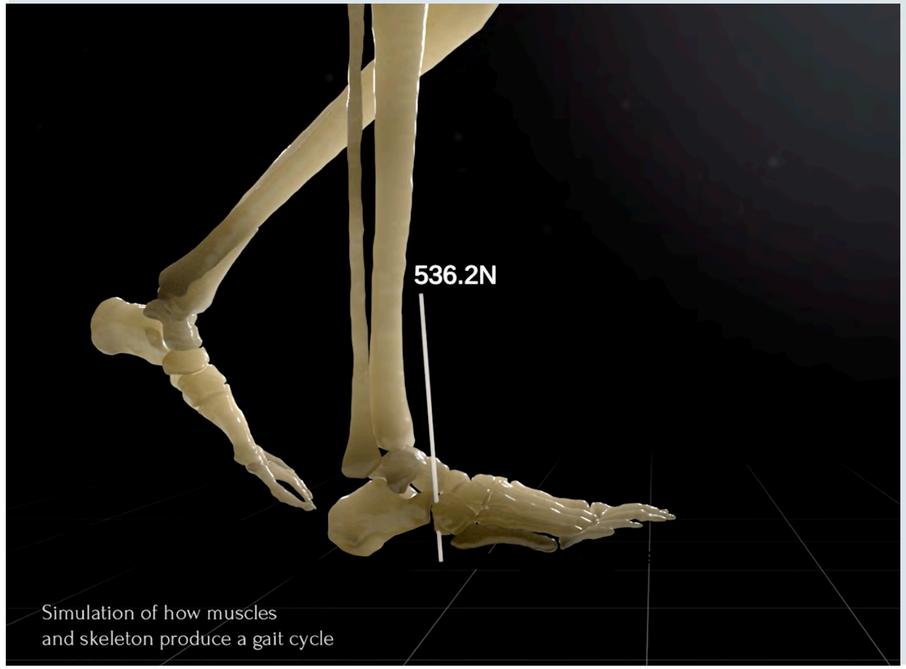

Beautiful **AND** accurate

- Have scientists and artists work together
- Convert data from scientific software/format into animation industry standards

Production pipeline

Typical pipeline in animation with a few extra steps for **DATA**

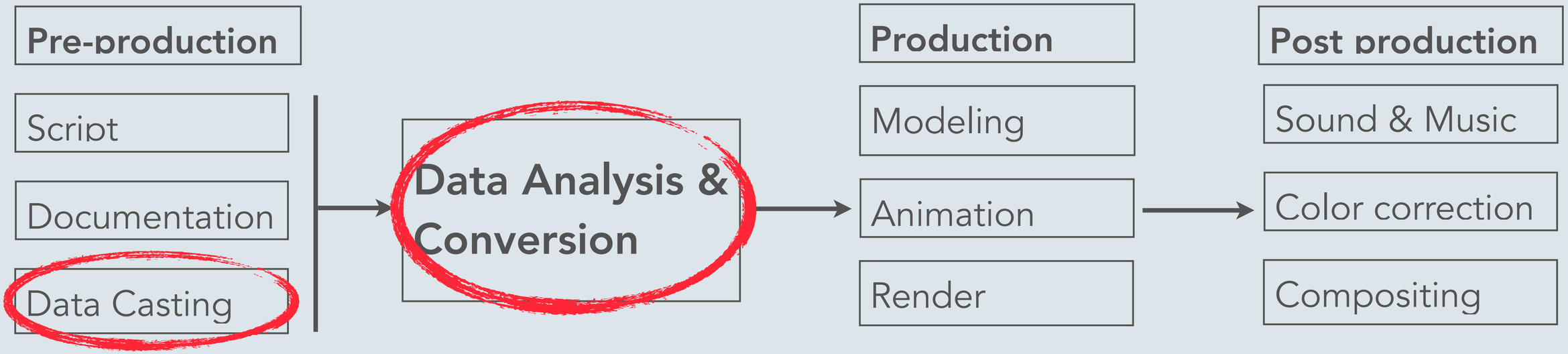

Production pipeline

Pre-production

Script

Documentation

Data Casting

Inspect data in Sci-Viz software

Data forensics if necessary

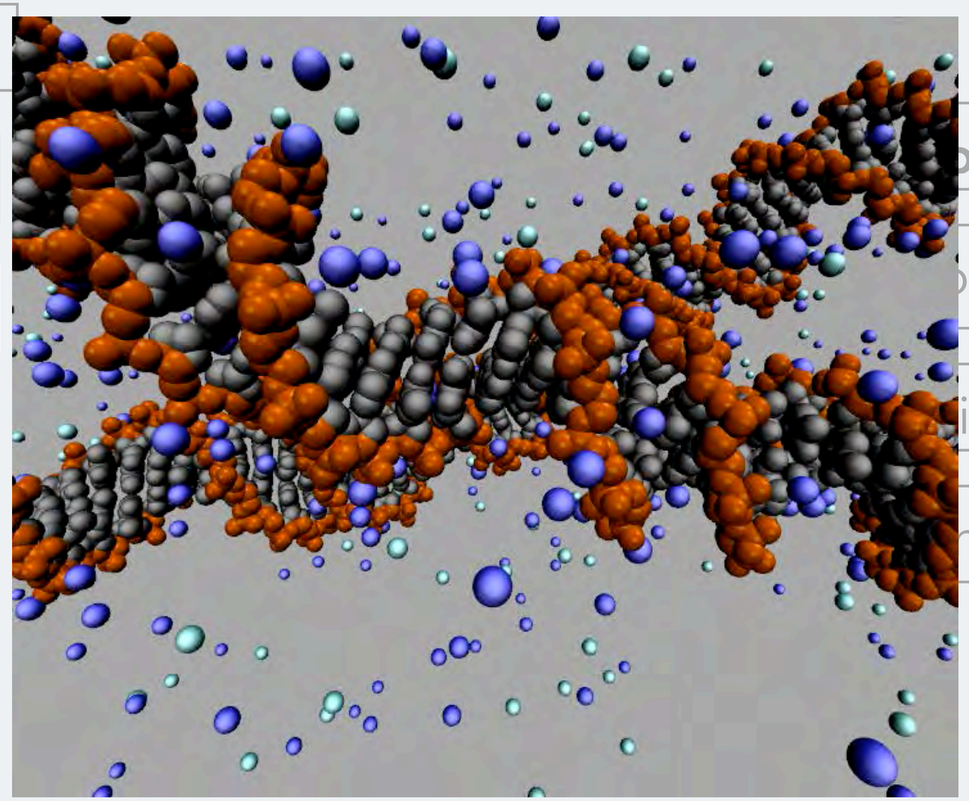

Harris, S. University of Leeds

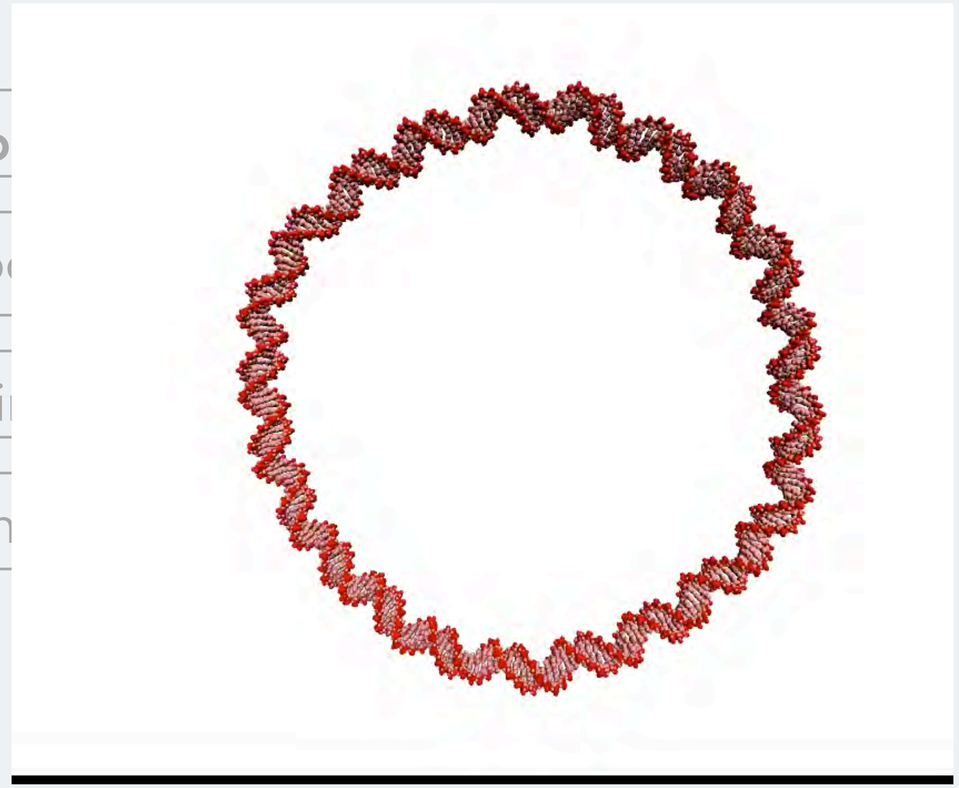

Pre-production

Script

Documentation

Data Casting

Inspect data in Sci-Viz software

Data forensics if necessary

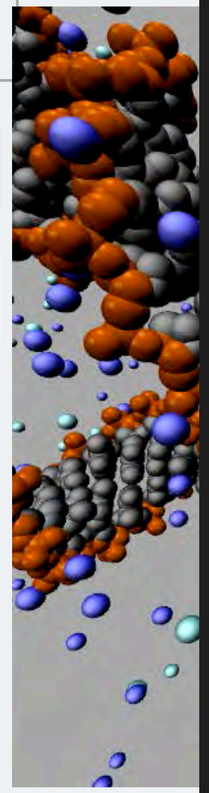

```
MODEL        1
COMPND    generated by VMD
AUTHOR    GENERATED BY OPEN BABEL 2.3.2
HETATM    1  C   LIG     1       4.788   5.645   1.595  1.00  0.00           C
HETATM    2  N   LIG     1       3.623   5.260   1.219  1.00  0.00           N
HETATM    3  N   LIG     1       5.883   5.527   0.897  1.00  0.00           N
HETATM    4  H   LIG     1       4.806   5.995   2.606  1.00  0.00           H
HETATM    5  H   LIG     1       2.739   5.511   1.733  1.00  0.00           H
HETATM    6  H   LIG     1       3.374   4.755   0.311  1.00  0.00           H
HETATM    7  H   LIG     1       5.979   5.189  -0.087  1.00  0.00           H
HETATM    8  H   LIG     1       6.726   5.991   1.213  1.00  0.00           H
HETATM    9  I   LIG     2       1.824   2.193   0.902  1.00  0.00           I
HETATM   10 PB   LIG     2       2.289   2.300   4.004  1.00  0.00          Pb
HETATM   11  I   LIG     1       5.566   2.669   3.757  1.00  0.00           I
HETATM   12  I   LIG     2       2.028   5.314   4.686  1.00  0.00           I
HETATM   13  C   LIG     3      12.190   5.479   1.021  1.00  0.00           C
HETATM   14  N   LIG     3      11.777   5.460  -0.223  1.00  0.00           N
HETATM   15  N   LIG     3      11.496   5.556   2.124  1.00  0.00           N
HETATM   16  H   LIG     3      13.253   5.263   1.099  1.00  0.00           H
HETATM   17  H   LIG     3      12.565   5.372  -0.960  1.00  0.00           H
HETATM   18  H   LIG     3      10.776   5.332  -0.452  1.00  0.00           H
HETATM   19  H   LIG     3      10.455   5.630   2.096  1.00  0.00           H
HETATM   20  H   LIG     3      12.004   5.448   2.976  1.00  0.00           H
HETATM   21  I   LIG     1       8.870   2.668   0.899  1.00  0.00           I
HETATM   22 PB   LIG     1       8.811   2.248   4.051  1.00  0.00          Pb
HETATM   23  I   LIG     1      11.804   1.664   4.270  1.00  0.00           I
HETATM   24  I   LIG     4       9.295   5.358   4.949  1.00  0.00           I
HETATM   25  C   LIG     5       5.330  12.094   1.660  1.00  0.00           C
HETATM   26  N   LIG     5       4.172  12.079   0.966  1.00  0.00           N
HETATM   27  N   LIG     5       6.496  12.373   1.187  1.00  0.00           N
HETATM   28  H   LIG     5       5.267  11.854   2.682  1.00  0.00           H
HETATM   29  H   LIG     5       3.346  11.780   1.489  1.00  0.00           H
HETATM   30  H   LIG     5       4.183  12.205  -0.030  1.00  0.00           H
HETATM   31  H   LIG     5       6.681  12.547   0.197  1.00  0.00           H
HETATM   32  H   LIG     5       7.313  12.287   1.792  1.00  0.00           H
HETATM   33  I   LIG     2       1.892   8.499   0.773  1.00  0.00           I
HETATM   34 PB   LIG     7       2.399   8.500   4.083  1.00  0.00          Pb
HETATM   35  I   LIG     7       5.391   8.633   3.508  1.00  0.00           I
HETATM   36  I   LIG     7       2.450  11.625   4.455  1.00  0.00           I
HETATM   37  C   LIG     8      11.365  10.941   0.807  1.00  0.00           C
HETATM   38  N   LIG     8      11.242  11.360   2.078  1.00  0.00           N
HETATM   39  N   LIG     8      11.028  11.621  -0.264  1.00  0.00           N
```

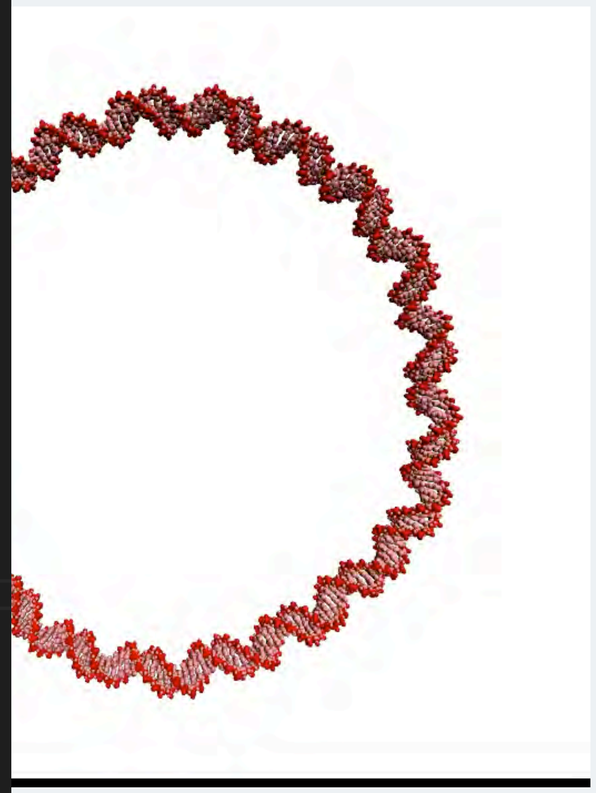

Production pipeline

Typical pipeline in film industry with a few extra steps for **DATA**

Pre-production

- Script
- Documentation
- Data Casting

Data Analysis & Conversion

Production

- Modeling
- Animation
- Render

Post production

- Sound & Music
- Color correction
- Compositing

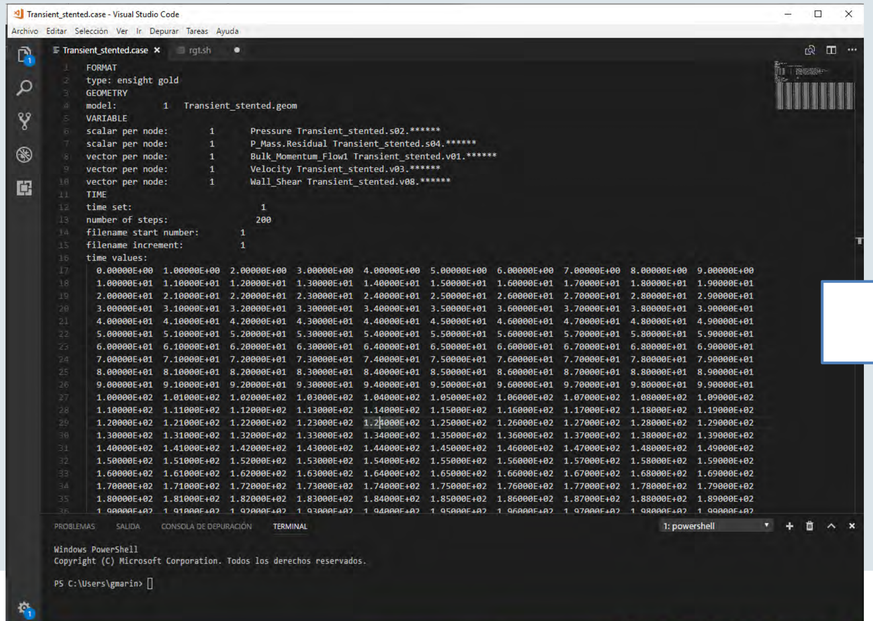

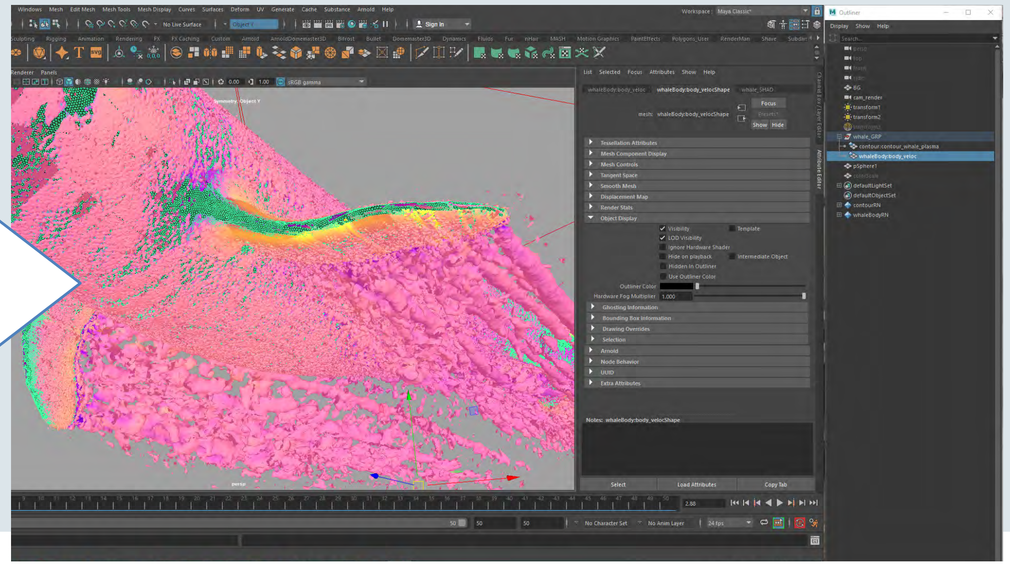

Data conversion workflow

Formats we can **read**

Standard formats

netcdf (climate)

vtk (engineering, physics, etc)

ensi (same as above)

PDB (molecular data)

csv

Almost anything readable by Paraview

Other formats

Structured and Unstructured Grids

Semi-Structured Grid Data

Generic Particle Data

Tables, trees, matrices

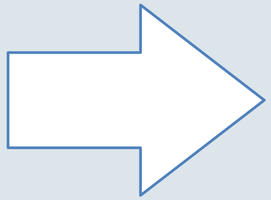

3D computer graphics software

Maya

Blender

3DSMax

Houdini

Renderers

Arnold Render

Renderman

Redshift

Blender Cycles

Data conversion workflow

Formats we can **write**

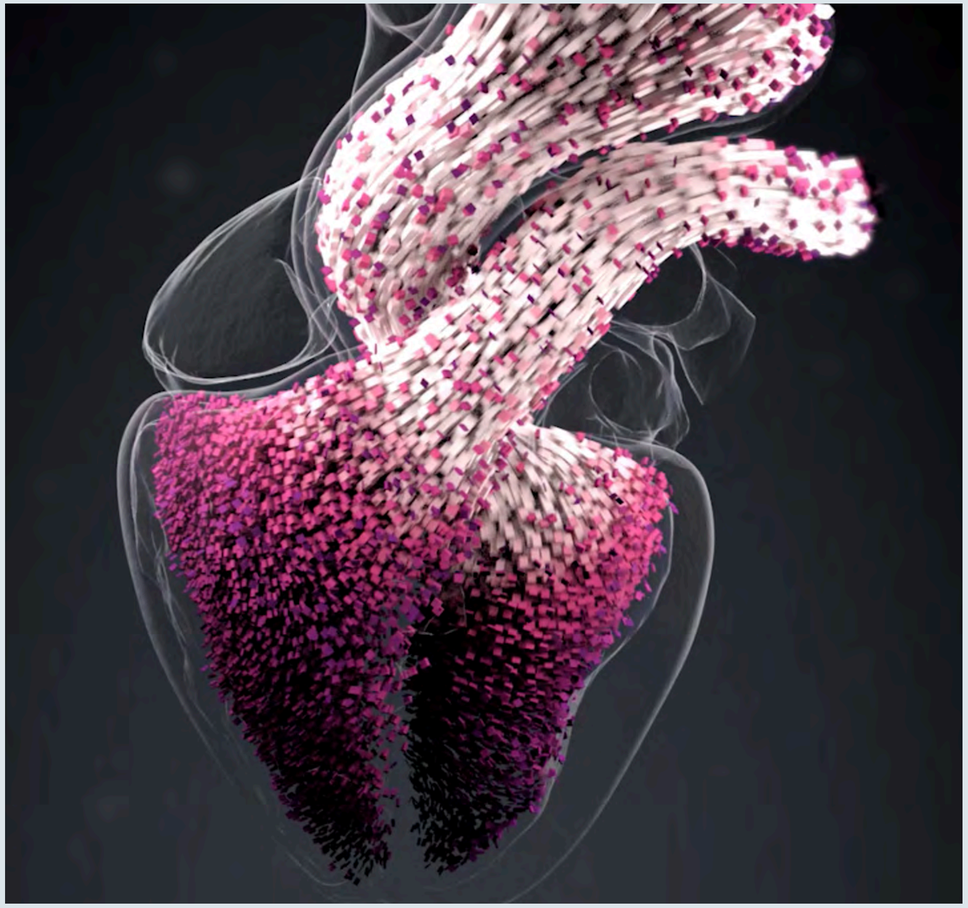

Volumetric data

Maya cache (mc)

Blender Voxels (bvox)

OpenVDB

Surface data

STL

OBJ

FBX

Alembic, etc…

Point/vector data

Maya cache (mc)

Partio

http://ytini.com/

Naiman, J.P., Borkiewicz, K., & Christensen, A.J. 2017, PASP, 129, 058008

A set of tools to read and write volumetric data

3D design software

- Maya: High cost but stable, easy to find experts
- Blender: Cheap (as in free) but less stable
  workflow is less “professional”
  very flexible, good for scientists
- Houdini: Procedural workflow,
  handles bigger datasets more efficiently

- Arnold Render: Biased, CPU renderer, really fast
- Renderman
- Redshift: Unbiased GPU-based, even faster
- Cycles: Unbiased render, good use of GPU cluster

3D computer graphics software

Maya
Blender
3DSMax
Houdini

Renderers

Arnold Render
Renderman
Redshift
Blender Cycles

Medtronic

- Commissioned film
- 10th Anniversary of the Pipeline Embolization Device
- Shown at LINNC 2019 (Live Interventional Neuroradiology & Neurosurgery Course)
- Audience mainly MDs
- 3D stereoscopic and Mono versions
- Coordinated by Dr. Ana Paula Narata; Simulations by Dr. Alberto Marzo

Inserm

Universidade Federal do ABC

CONICET

The University Of Sheffield.

Intro: Patient-based geometry of intracranial artery

1

2

CFD study of the blood flow before stent implantation

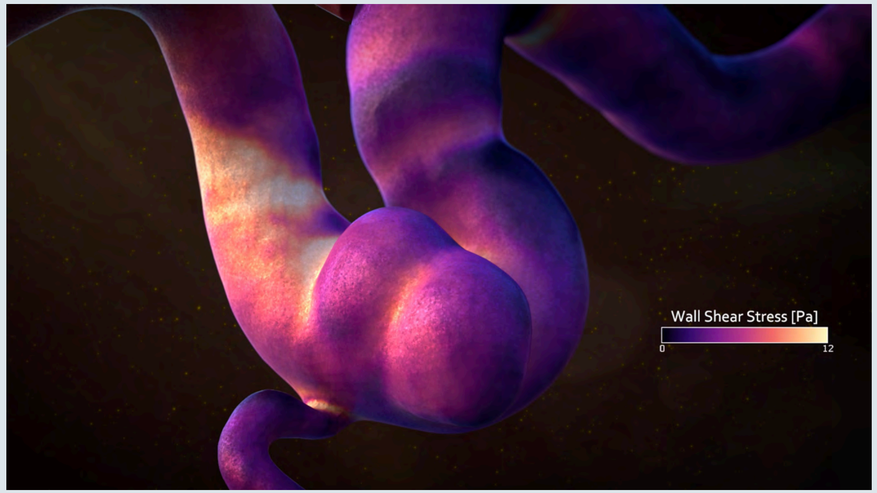

CFD study of the blood flow after stent implantation

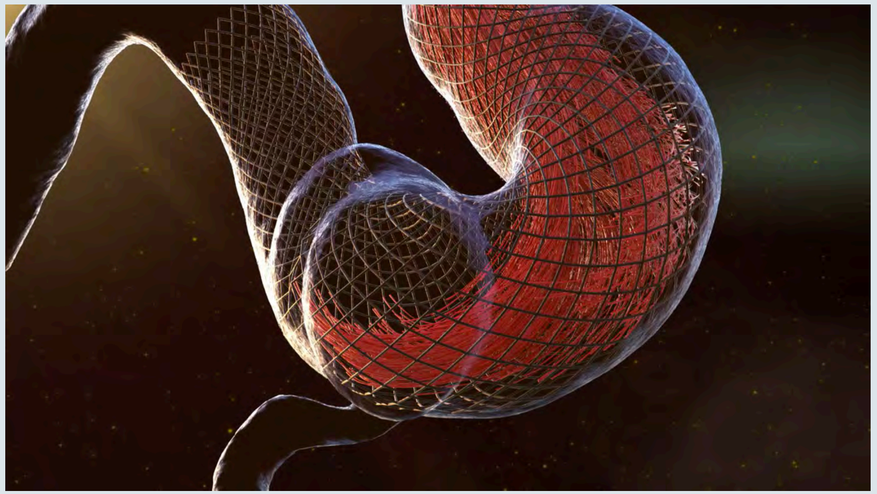

4

3

Accurate recreation of the stent delivery process

CFD study references

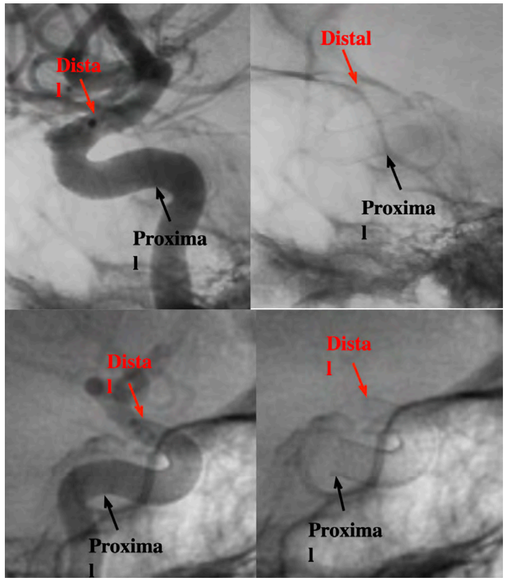

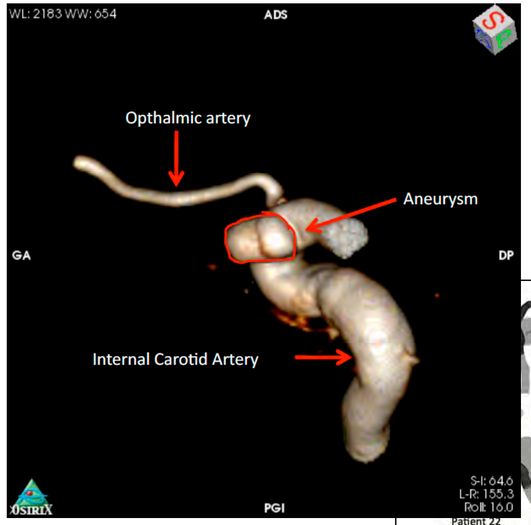

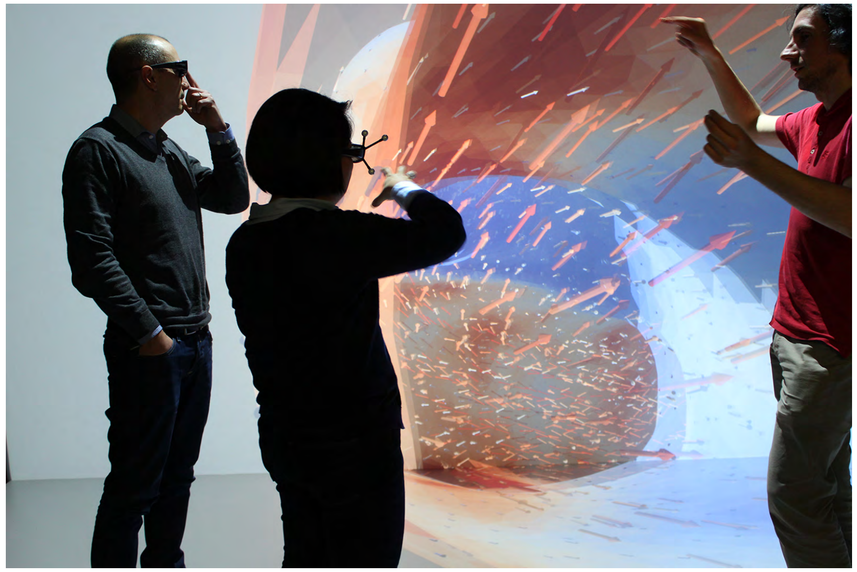

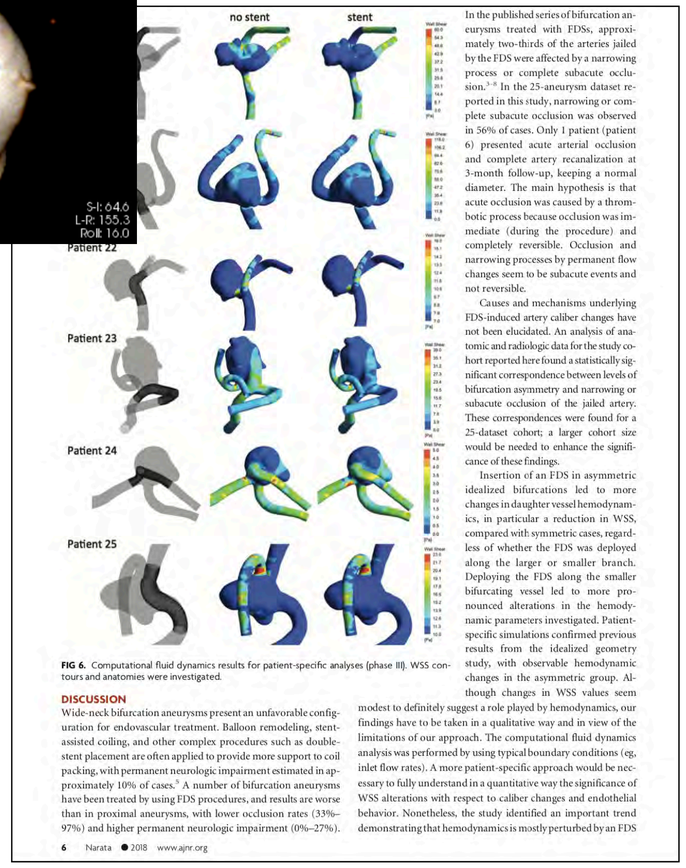

FIG 6. Computational fluid dynamics results for patient-specific analyses (phase III). WSS contours and anatomies were investigated.

DISCUSSION

Wide-neck bifurcation aneurysms present an unfavorable configuration for endovascular treatment. Balloon remodeling, stent-assisted coiling, and other complex procedures such as double-stent placement are often applied to provide more support to coil packing, with permanent neurologic impairment estimated in approximately 10% of cases.[5] A number of bifurcation aneurysms have been treated by using FDS procedures, and results are worse than in proximal aneurysms, with lower occlusion rates (33%–97%) and higher permanent neurologic impairment (0%–27%).

In the published series of bifurcation aneurysms treated with FDSs, approximately two-thirds of the arteries jailed by the FDS were affected by a narrowing process or complete subacute occlusion.[7,8] In the 25-aneurysm dataset reported in this study, narrowing or complete subacute occlusion was observed in 56% of cases. Only 1 patient (patient 6) presented acute arterial occlusion and complete artery recanalization at 3-month follow-up, keeping a normal diameter. The main hypothesis is that acute occlusion was caused by a thrombotic process because occlusion was immediate (during the procedure) and completely reversible. Occlusion and narrowing processes by permanent flow changes seem to be subacute events and not reversible.

Causes and mechanisms underlying FDS-induced artery caliber changes have not been elucidated. An analysis of anatomic and radiologic data for the study cohort reported here found a statistically significant correspondence between levels of bifurcation asymmetry and narrowing or subacute occlusion of the jailed artery. These correspondences were found for a 25-dataset cohort; a larger cohort size would be needed to enhance the significance of these findings.

Insertion of an FDS in asymmetric idealized bifurcations led to more changes in daughter vessel hemodynamics, in particular a reduction in WSS, compared with symmetric cases, regardless of whether the FDS was deployed along the larger or smaller branch. Deploying the FDS along the smaller bifurcating vessel led to more pronounced alterations in the hemodynamic parameters investigated. Patient-specific simulations confirmed previous results from the idealized geometry study, with observable hemodynamic changes in the asymmetric group. Although changes in WSS values seem modest to definitely suggest a role played by hemodynamics, our findings have to be taken in a qualitative way and in view of the limitations of our approach. The computational fluid dynamics analysis was performed by using typical boundary conditions (eg, inlet flow rates). A more patient-specific approach would be necessary to fully understand in a quantitative way the significance of WSS alterations with respect to caliber changes and endothelial behavior. Nonetheless, the study identified an important trend demonstrating that hemodynamics is mostly perturbed by an FDS

The University Of Sheffield. INSIGNEO Institute for in silico Medicine université de TOURS

CFD Reveals Changes in Velocity and Wall Shear Stress

Computational fluid dynamics (CFD) modelling within cardiovascular medicine is a specialist area of mathematics , used routinely across a diverse range of safety-critical engineering systems. CFD modelling has already revolutionised the research and development of devices such as stents, valve prostheses, and ventricular assist devices by facilitating rapid, economical and low-risk prototyping when combined with cardiovascular imaging. It enables detailed characterisation of complex physiological pressure and flow fields and the computation of metrics that cannot be directly measured, for example, wall shear stress, of particular interest in clinical applications.

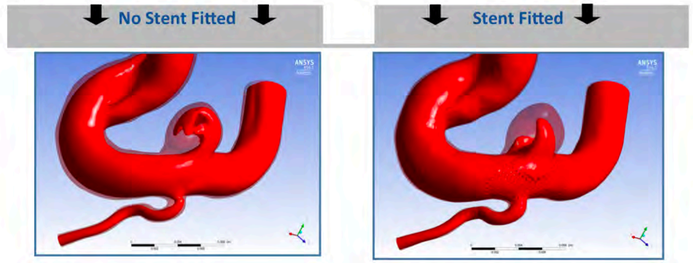

Velocity Iso-surface: Surface plots showing areas of higher velocity (jets) entering the aneurysm sac in the untreated (left) and treated (right) case using a typical flow diverting stent (FDS) geometry in a patient-specific ophthalmic artery bifurcation.

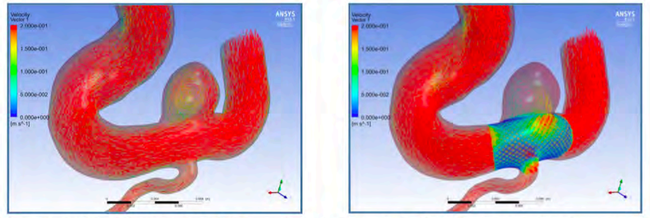

Velocity Vectors: Vector plots of the velocity field showing direction and magnitude of blood flow entering and circulating within the aneurysm before (left) and after (right) treatment with FDS

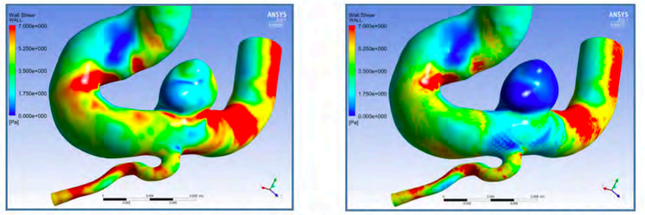

Wall Shear Stress: Contour plots of Wall Shear Stress before (left) and after (right) treatment with FDS showing significant alteration of aneurysm sac haemodynamics with little effect on the haemodynamics of the surrounding vasculature.

CFD study references

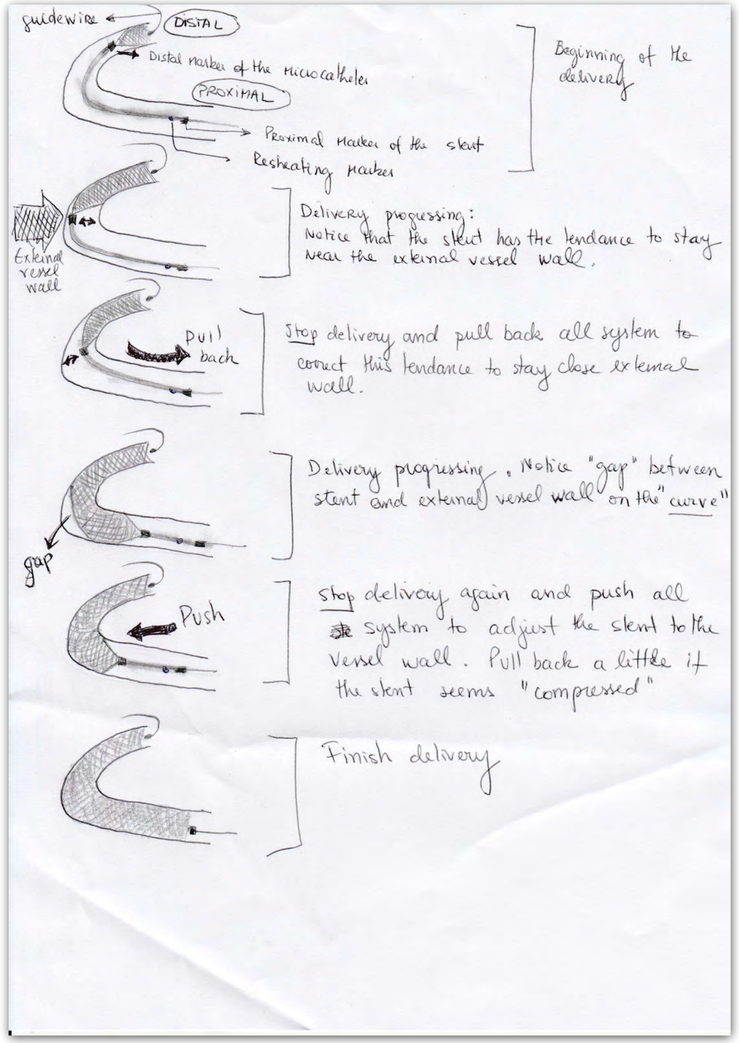

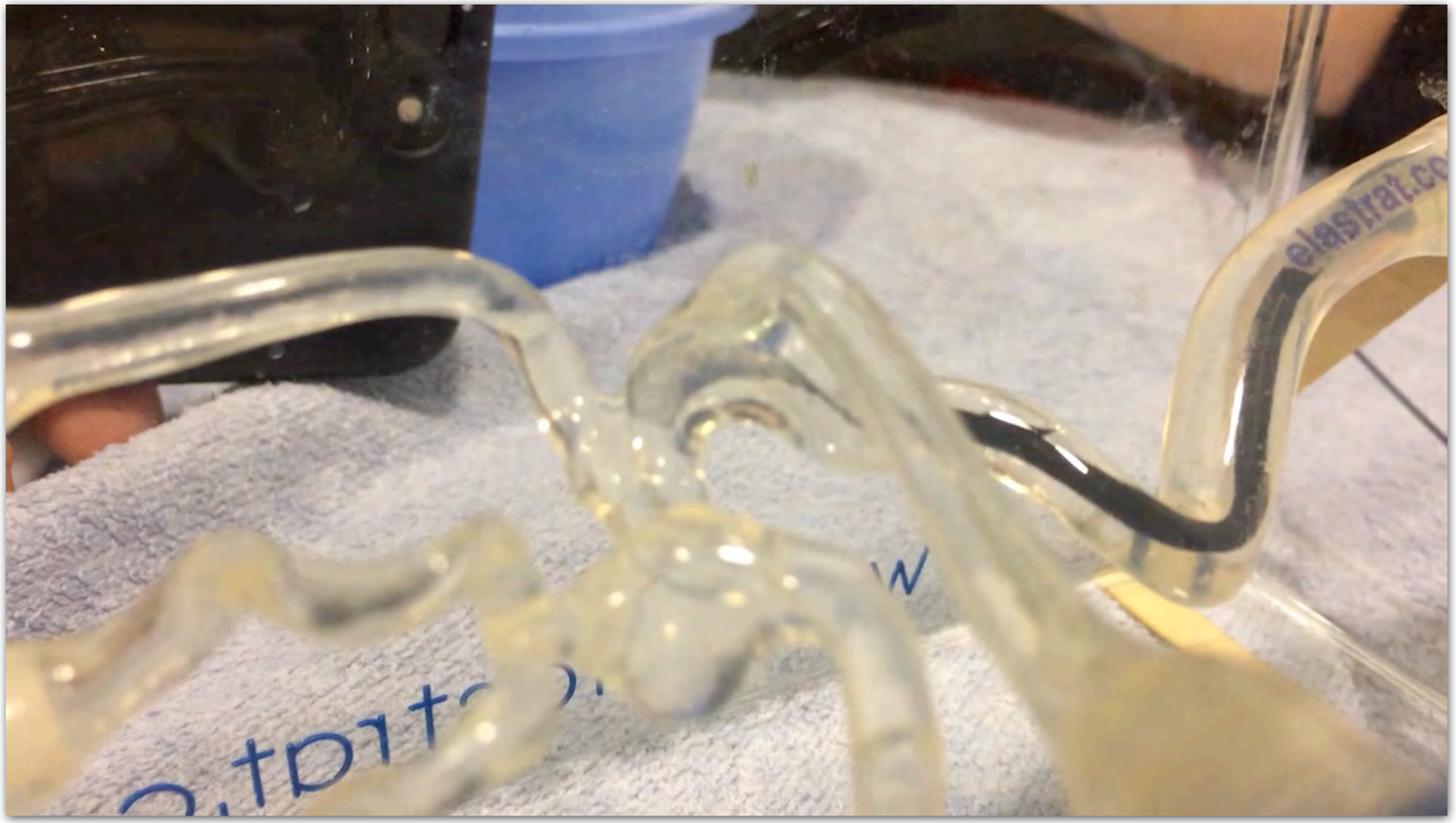

Thanks!